



## Article

# On the Potential of RST-FLOOD on Visible Infrared Imaging Radiometer Suite Data for Flooded Areas Detection

Teodosio Lacava <sup>1,\*</sup>, Emanuele Ciancia <sup>2</sup>, Mariapia Faruolo <sup>1</sup>, Nicola Pergola <sup>1</sup>,  
Valeria Satriano <sup>1</sup> and Valerio Tramutoli <sup>2</sup>

<sup>1</sup> National Research Council, Institute of Methodologies for Environmental Analysis, C. da S. Loja, 85050 Tito Scalo (PZ), Italy; mariapia.faruolo@imaa.cnr.it (M.F.); nicola.pergola@imaa.cnr.it (N.P.); valeria.satriano@imaa.cnr.it (V.S.)

<sup>2</sup> University of Basilicata, School of Engineering, Via dell'Ateneo Lucano, 10, 85100 Potenza, Italy; emanuele.ciancia@imaa.cnr.it (E.C.); valerio.tramutoli@unibas.it (V.T.)

\* Correspondence: teodosio.lacava@imaa.cnr.it; Tel.: +39-0971427242; Fax: +39-0971427205

Received: 13 February 2019; Accepted: 7 March 2019; Published: 12 March 2019



**Abstract:** Timely and continuous information about flood spatiotemporal evolution are fundamental to ensure an effective implementation of the relief and rescue operations in case of inundation events. In this framework, satellite remote sensing may provide a valuable contribution provided that robust data analysis methods are implemented and suitable data, in terms of spatial, spectral and temporal resolutions, are employed. In this paper, the Robust Satellite Techniques (RST) approach, a satellite-based differential approach, already applied at detecting flooded areas (and therefore christened RST-FLOOD) with good results on different polar orbiting optical sensors (i.e., Advanced Very High Resolution Radiometer – AVHRR – and Moderate Resolution Imaging Spectroradiometer – MODIS), has been fully implemented on time series of Suomi National Polar-orbiting Partnership (Suomi-NPP-SNPP) Visible Infrared Imaging Radiometer Suite (VIIRS) data. The flooding event affecting the Metaponto Plain in Basilicata and Puglia regions (southern Italy) in December 2013 was selected as a case study and investigated by analysing five years (only December month) of VIIRS Imagery bands at 375 m spatial resolution. The achieved results clearly indicate the potential of the proposed approach, especially when compared with a satellite-based high resolution map of flooded area, as well as with the official flood hazard map of the area and the outputs of a recent published VIIRS-based method. Both flood extent and dynamics have been recognized with good reliability during the investigated period, with only a residual 11.5% of possible false positives over an inundated area extent of about 73 km<sup>2</sup>. In addition, a flooded area of about 18 km<sup>2</sup> was found outside the hazard map, suggesting it requires updating to better manage flood risk and prevent future damages. Finally, the achieved results indicate that medium-resolution optical data, if analysed with robust methodologies like RST-FLOOD, can be suitable for detecting and monitoring floods also in case of small hydrological basins.

**Keywords:** flood; satellite remote sensing; near real time; RST-FLOOD; SNPP; JPSS; VIIRS

## 1. Introduction

Among natural hazards, floods are currently the most frequent and costliest [1], causing worldwide fatalities as well as huge economic damage, affecting both rural and urban environments [2]. For instance, in 2017, 47% of the economic losses due to natural catastrophes were specifically related to floods (including both river flooding and flash floods) and another 35% to meteorological (i.e., storms) events [3]. Moreover, flood risk and the associated losses are projected to significantly increase in the

future due to both human activities (i.e., land use/cover changes, new infrastructures construction, etc.) and natural causes (i.e., the effects of climate change, subsidence, etc.) [2,4,5]. To reduce the effects of these potential threats, effective flood risk management is required [2] as well as, in case of disaster, a prompt detection of flooded areas in order to support decision makers with relief and rescue operations [6]. In this framework, satellite remote sensing data have become a powerful tool, thanks to the growing availability of several satellite/sensors systems able to provide different information about inland surface water presence useful to manage flooding events [7,8].

Microwave sensors can provide useful evidence (i.e., 24 hours and under cloudy conditions) about flooded areas, with different characteristics depending on the specific technology used [9]. Active systems, such as Synthetic Aperture Radar (SAR), can furnish data at a high spatial resolution (up to few meters) but, generally, with a long revisit period (up to five to six days), hence often resulting not suitable for assuring a quick identification and a continuous monitoring of flood-inundated area [10,11]. Their capabilities greatly improve when national space agencies focus the acquisitions of their satellites on the affected area or when specific services, such as the International Charter Space and Major Disasters [12] or the Copernicus Emergency Management [13] are activated. On the other hand, passive microwave sensors allow acquiring data with a poor spatial resolution (up to tens of kilometres) but with a high temporal frequency (up to few hours), especially if considering those instruments on board of polar weather satellites constellation [14]. Their spatial and temporal resolution makes these sensors particularly suitable for studying large-scale floods [6] but less adequate in case of moderate/small size events.

Optical sensors, acquiring data in the visible (VIS), near infrared (NIR) and shortwave infrared (SWIR) bands, allow for the detection of flooded areas during daytime and in absence of clouds [7,10]. The spatial resolution of these data ranges from few to hundreds of meters while the temporal resolution from some hours to a few days [10,15–17]. Therefore, in order to ensure continuous and near real time information in daytime conditions about flood dynamics, optical sensors onboard weather polar satellites represent one of the most suitable solution in furnishing useful data, in terms of both spatial, spectral and temporal resolutions [18]. Furthermore, considering that both optical and microwave sensors are often present on these satellites, their integration is an added value in providing a more comprehensive overview of the ongoing phenomena [6,18–20].

In the last years, optical data acquired by the Advanced Very High Resolution Radiometer (AVHRR) and Moderate Resolution Imaging Spectroradiometer (MODIS) have been analysed by implementing the Robust Satellite Technique (RST) [21] for detecting flooded areas and therefore christened RST-FLOOD, with satisfactory results [22,23]. In this paper, RST-FLOOD has been applied to Suomi National Polar-orbiting Partnership (Suomi-NPP) (SNPP) Visible Infrared Imaging Radiometer Suite (VIIRS) imagery to analyse the flooding event which hit the Basilicata and Puglia regions (southern Italy) in the first week of December 2013. The main objective of this work is to assess the potential of the developed RST-FLOOD scheme, when implemented on VIIRS Imagery (at 375 m of spatial resolution) bands, to get useful and reliable information for small-scale flood events.

## 2. The Test Case

The selected Region of Interest (ROI) is the Metaponto plain area, located between the south-eastern corner of the Basilicata Region (southern Italy) and a subset of the Puglia Region (Figure 1). This plain is of particular socio-economic and environmental importance for the region and interested by degradation processes mainly linked to land management and soil characteristics [24,25]. The area encloses the terminal sector of all the main Basilicata river basins, namely Sinni, Agri, Cavone, Basento and Bradano and of the Lato River, the major one of the Puglia Region (Figure 1).

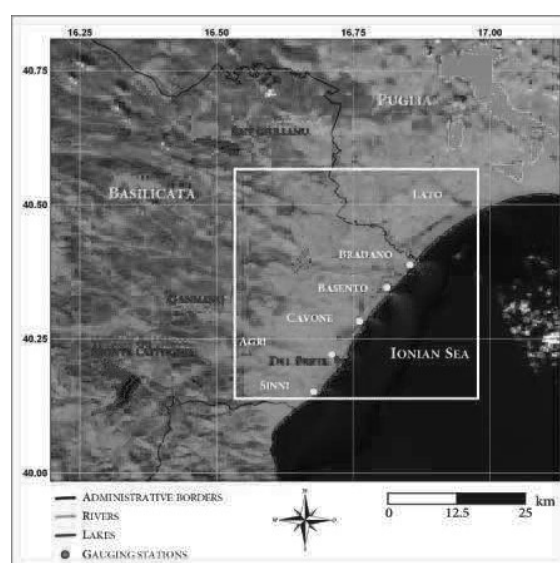


**Figure 1.** Localization of the Region of Interest (red box, in WGS-84 lat-long projection). In background the RGB False Colour (Red = Shortwave Infrared, namely I3 VIIRS band; Green = Near Infrared, namely I2 VIIRS band; Blue = RED, namely I1 VIIRS band) of VIIRS Imagery data acquired on 4 December 2013 at 12.10 GMT. Yellow dots indicate the localization of gauging stations along the five main rivers reaching the Ionian coast. The red segment and the white box will be used in the text.

All these rivers are strongly seasonal dependent, with maximum hydrometric levels recorded in winter and minimum in the summer [26]. The annual minimum flow rate of the Sinni and Agri rivers, whose basins are those mostly affected by precipitations at regional level, is 1.38 and 0.5 m<sup>3</sup>/s, respectively [27]. Lower values are instead recorded for the Bradano and Basento rivers (i.e., 0.04 and 0.08 m<sup>3</sup>/s), while Cavone River flow rate is practically nil [27]. The river levels are registered by the Civil Protection Department of Basilicata Region [28], by means of the five gauging stations (depicted by yellow dots in Figure 1) positioned close to the river mouths (i.e., within the Metaponto Plain), at the intersection with the freeway of the Basilicata region called "StradaStatale 106." Based on the temporal range when water levels were available (January 2011–September 2016), the three maxima measured at the five gauging stations and the corresponding dates are reported in Table 1, where they are listed from the highest to the lowest.

**Table 1.** The three maximum water levels (listed in decreasing order) measured in the period 01/01/2011–30/09/2016 and the corresponding dates for the Sinni, Agri, Cavone, Basento and Bradano rivers [28]. Note that for Agri River, data are available only for the period 01/01/2013–30/09/2016.

	Sinni	Agri	Cavone	Basento	Bradano
	3.59 m 01/12/2013	4.19 m 01/12/2013	5.22 m 04/02/2014	7.92 m 02/12/2013	6.04 m 02/03/2011
Max River Level Date	3.47 m 28/03/2015	3.93 m 13/03/2016	5.00 m 02/12/2013	7.81 m 03/12/2013	5.39 m 02/12/2013
	3.46 m 23/02/2012	3.55 m 02/12/2013	4.81 m 19/02/2011	7.60 m 02/03/2011	4.83 m 03/12/2013

Looking at the data in Table 1 it is worth noting an evident increase in the water level of all the rivers during the first week of December 2013 (Figure 2), which suggests the occurrence of an extreme hydrological event. The "Ciclone Nettuno" storm hit the Basilicata Region between 30 November and 3 December 2013, producing heavy convective precipitation [29,30]. A daily precipitation value of 130 mm was recorded on 1 December at the Bradano River gauging station, with a cumulative

one of 200 mm for the entire event [31], indicating the strong intensity of this meteorological event. The consequent flooding event affected not only the Metaponto Plain in the Basilicata Region but also some areas in Puglia, where the Lato River overflowed near Castellaneta Marina, causing the closure of the freeway “Strada Statale 106” and severe damage to the surrounding lands and villages [28,32–36].

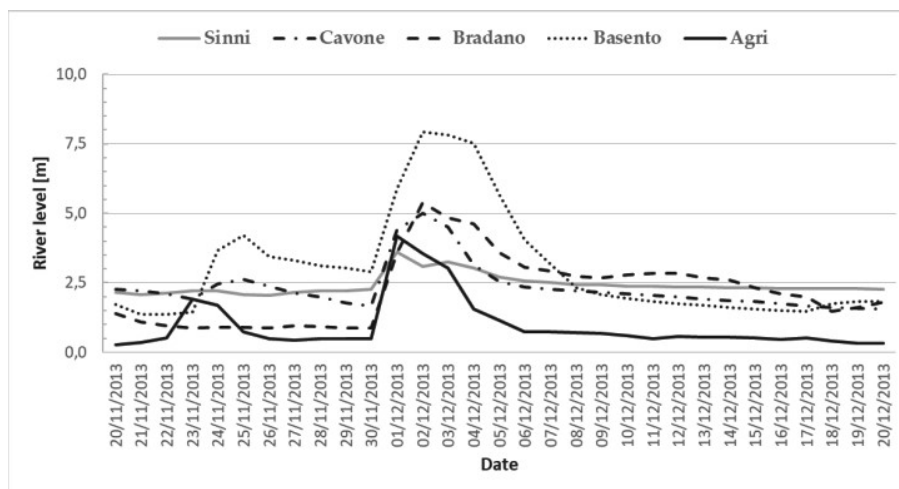


**Figure 2.** Basilicata river levels measured in the period 20/11/2013–20/12/2013 at the correspondent gauging stations indicated in Figure 1 [28].

This event has been already investigated by Reference [31], which, by integrating multi-temporal COSMO Sky MED SAR intensity images and interferometric-SAR coherence data with geomorphic and other ground information within a Bayesian network, detected flooded area, reaching accuracies of up to 89%, in the 2–3 December 2013 period focusing on a small subset of Figure 1 centred on the Bradano River mouth. [37] extended the work of Reference [31] adding to the two above-mentioned COSMO Sky Med SAR imagery a Pléiades-1B High-Resolution data of 5 December 2013 to investigate a limited portion of Figure 1 centred on the Basento River mouth. SAR data were processed and used as in Reference [31] to identify flooded area on the above-mentioned days, while the Normalized Difference Vegetation Index (NDVI) was implemented on the Pléiades image to highlight water presence at the end of the event. A visual interpretation of the optical data combined with a field campaign allowed inferring information about results uncertainties [37]. Concerning the selected test case, the integration of outcomes of these two previous works gives an overview of the flood effects in a very small area (e.g., about 20 km<sup>2</sup>) and for a short temporal range (up to four days).

The approach proposed in this work should allow for both the extension of the spatiotemporal domain of the investigation of the event and the deep analysis of the phenomenon, thanks to the large swath as well as the continuity of observation ensured by sensors on-board polar satellites, like VIIRS.

### 3. Data and Methods

#### 3.1. VIIRS Data

The VIIRS sensor is currently operational onboard SNPP (since October 2011) and the US Joint Polar Satellite System 1 (JPSS-1 or NOAA-20, since November 2017). In addition, three more VIIRS sensors will fly on the follow-on JPSS2-JPSS4 satellites, planned for launch from 2021 to 2031 [38,39] assuring an operational continuity like the one already offered by AVHRR and MODIS, namely its predecessors. Thanks to its large swath (i.e., 3060 km), VIIRS has been providing a daily full Earth coverage [40], collecting data in 22 different spectral bands of the electromagnetic spectrum, ranging from 0.412  $\mu\text{m}$  and 12.01  $\mu\text{m}$ , with a spatial resolution of 750 m at the nadir for both the Day/Night panchromatic Band (DNB) and the 16 Moderate resolution bands (M-bands) and of 375 m for the 5 high-resolution Imagery bands (I-bands) [40].

In this work, the following I-bands, namely I1 (0.60–0.68  $\mu\text{m}$ , RED), I2 (0.85–0.88  $\mu\text{m}$ , Near Infrared-NIR), I3 (1.58–1.64  $\mu\text{m}$ , Shortwave Infrared-SWIR) and I5 (10.5–12.4  $\mu\text{m}$ , Thermal Infrared-TIR) acquired in the month of December from 2013 to 2017 (for a total of 171 SNPP orbits) were analysed. In addition, the I-band terrain-corrected geolocation data (GITCO), including longitude, latitude, solar zenith angles, solar azimuth, sensor zenith and sensor azimuth angles, were also exploited. The I1–I3 data were converted in reflectance (R) values, while those related to I5 band in brightness temperature (BT).

In more detail, SNPP Sensor Data Record (SDR) data, directly acquired at the satellite receiving station of the Institute of Methodology for Environmental Analysis (IMAA) located in Tito Scalo (Basilicata region, southern Italy), have been processed by running the Community Satellite Processing Package (CSPP). Furthermore, SDR data were downloaded from NOAA CLASS archive [41] to fill any gaps within the considered historical series. The Polar2Grid v2.2 software [42] allowed the SDR spatial sub-setting over the ROI.

A total of 684 VIIRS SDR data was collected for the study area of  $601 \times 600$  pixels, shown in Figure 1. The cloud-free VIIRS daytime imagery of the event, acquired on 4,5,6,7 and 8 December 2013, at 12.10 GMT, 11.52 GMT, 11.35 GMT, 11.12 GMT and 12.36 GMT, respectively, have been processed in terms of RST-FLOOD to analyse the above mentioned flooding event.

### 3.2. Ancillary Data

The reliability of the RST-FLOOD results has been assessed by means of a high resolution map, carried out applying a change detection scheme to a Landsat 7 (Enhanced Thematic Mapper Plus) ETM+ data (Figure 3) and the flood hazard maps provided, for the studied area, by the Italian Ministry of the Environment and Land Protection [43] (Figure 4). In addition, the sensitivity of the achieved outcomes has been evaluated for comparison with the outputs of the VIIRS NOAA&GMU Flood Version 1.0 (VNG Flood V1.0, hereafter VNG) software, recently distributed in the framework of the CSPP network [44] (Figure 5).

Two Landsat 7 ETM+ (scene of  $2534 \times 3400$  pixels, at 30 m of spatial resolution) images provided over the ROI with a higher spatial resolution than VIIRS ones, have been used to evaluate the flood detection results. In detail, the Landsat 7 ETM+ images acquired on 5 December 2013, at 9.31 GMT and 24 December 2014, at 9.33 GMT were combined in a change detection scheme to highlight the flooded area. The Landsat Level-1 data, downloaded from USGS Earth Explorer Earth website [45], are distributed as scaled and calibrated digital numbers (DN). In this work, the DNs were converted to calibrated TOA (Top Of Atmosphere) reflectances using metadata which are distributed with the product. In Figure 3a,b the false colour composite images (R = Band 7, SWIR, 2.09–2.35  $\mu\text{m}$ ; G = Band 5, SWIR, 1.55–1.75  $\mu\text{m}$ ; B = Band 1, RED, 0.63–0.69  $\mu\text{m}$ ) of the analysed imagery are shown. The 753 combination provides a “natural-like” rendition, where flooded areas should look very dark blue or black [46]. Looking at the images, the presence of a large number of blue pixels is evident for the one acquired concurrently with the 2013 flood event (Figure 3a), while the other should more reflect the unperturbed condition. Besides, for each image, three maps were produced: RED – SWIR (B3 – B5), RED/SWIR (B3/B5) and their normalized difference (NDSI =  $\text{RED} - \text{SWIR}$ ,  $\text{RED}/\text{SWIR}$ ,  $\text{B3} - \text{B5}/\text{B3} + \text{B5}$ ), which all should be affected by a variation in surface water presence, as better discussed later (see Section 3.3). The “water affected areas,” shown in magenta in Figure 3c (re-projected at 375 m, for the comparison with RST-FLOOD results), is the “and” combination of the detections carried out integrating these three maps. By this approach, an area of about 24 km<sup>2</sup> has been estimated as flooded affected, mostly localized along the Basento, Bradano and Lato rivers. Such a value is likely underestimated because of a number of issues regarding Landsat data [47], like the presence of data gaps towards the edges of the images due to the striping caused by the failure of the Landsat-7 ETM+ scan line corrector (SLC) in 2003.

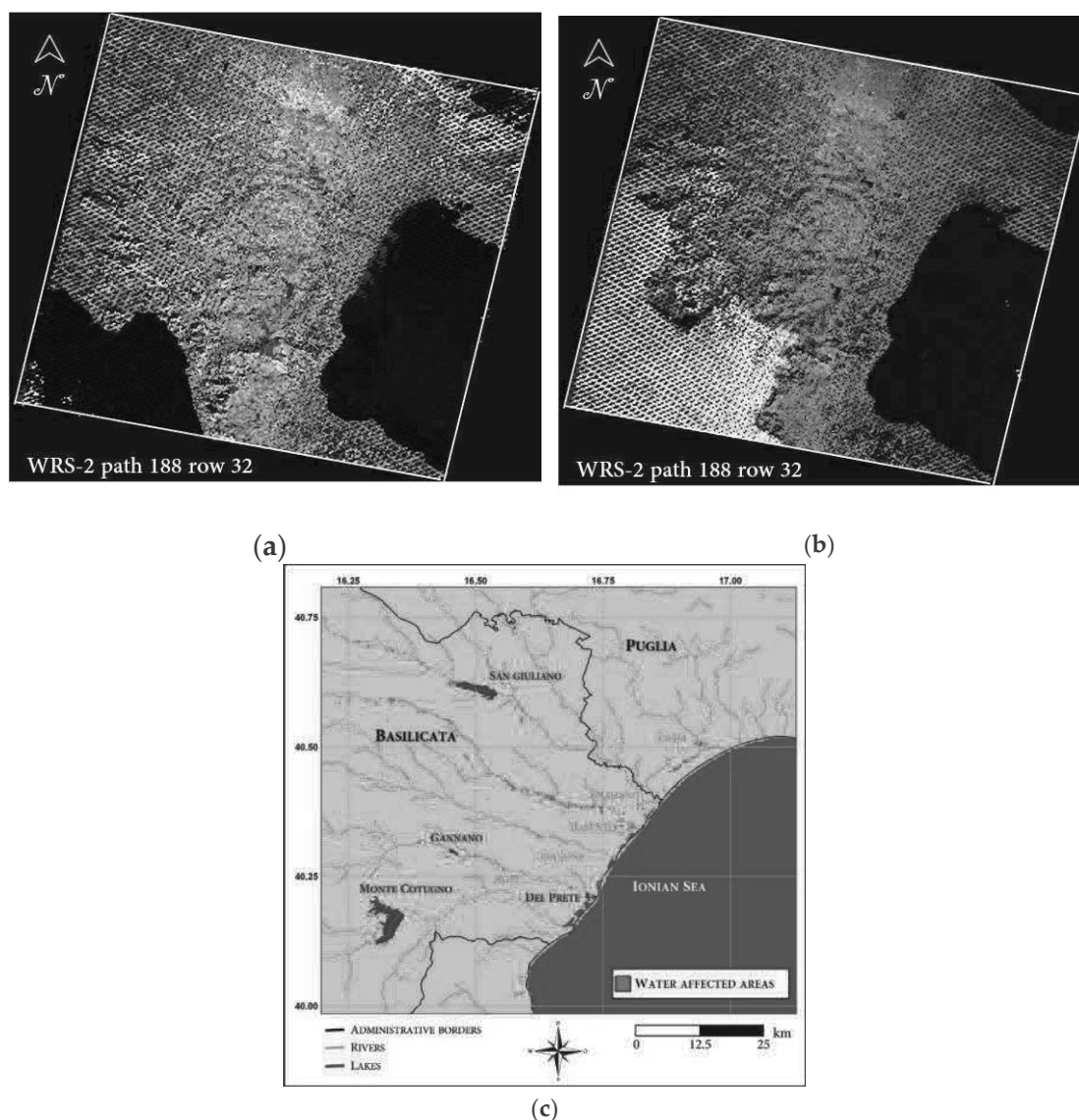


**Figure 3.** The Landsat 7 ETM+ false-colour (R = Band 7, Shortwave Infrared, 2.09–2.35  $\mu\text{m}$ ; G = Band 5, Shortwave Infrared, 1.55–1.75  $\mu\text{m}$ ; B = Band 1, Blue, 0.45–0.52  $\mu\text{m}$ ) composite image of (a) 05/12/2013 at 9.31 and (b) 24/12/2014 at 9.33 GMT; (c) change detection map showing the water affected areas, depicted in magenta, over the region of interest (ROI).

In Italy, the Ministry of the Environment and Land Protection plans finances and controls the actions aimed at the hydrogeological risk reduction. In this framework, the Hydro-Geologic Safety Plan (named hereafter PAI) is drawn up for each river basin. In the Basilicata PAI, produced by the Basilicata Inter-Regional Basin Authority, through hydrological and hydraulic studies carried out by the University of Basilicata [48], three areas of fluvial pertinence in relation to flood risk as well as in relation to the natural water path have been defined as areas of probable flood risk [48]. Such zones are established according to the three following scenarios: i) frequently occurring flood events (high probability, likely return period 30–50 years); ii) less frequently occurring flood events (medium probability, likely return period 100–200 years); iii) extreme flood events (low probability, likely return period 300–500 years). The last ones, delivered by the Italian national geoportal [43] and updated at December 2016, are provided in Web Map Service (WMS) format. The PAI referring to the ROI is shown in Figure 4, where the lighter the colour (from black to yellow) the lower the probability of the occurrence of extreme floods.

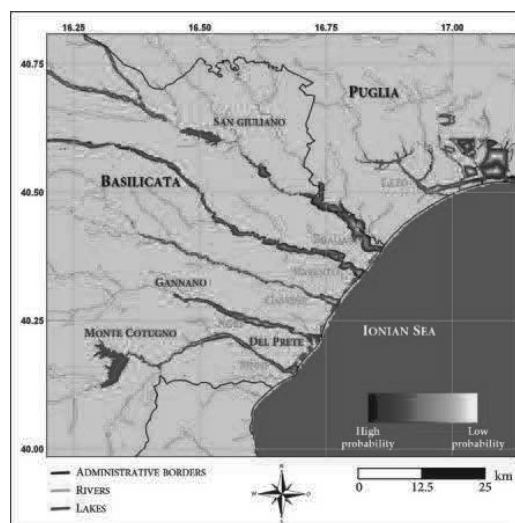


**Figure 4.** The flood hazard map (PAI) for the ROI. Areas are depicted according to the palette, ranging from black to yellow when the return period increases.

The VNG is a satellite-based flood extent product developed using SNPP/VIIRS imagery to derive near real-time flood maps for the National Weather Service (NWS) River Forecast Centres (RFC) in the USA [11]. It exploits a multi-step (decision trees) approach based on SNPP/VIIRS imagery to automatically generate near real-time flood maps in any land region between 80 °S and 80 °N [11]. Geolocation (GITCO) and VIIRS data, such as the SNPP/VIIRS 750-m resolution cloud mask intermediate product (IICMO) and M-band terrain-corrected geolocation data (GMTCO) are also used in combination with several static ancillary datasets (e.g., global land cover, global land and water masks, digital elevation models, etc.). These data are integrated into the VNG software, using fixed threshold, contextual and change detection approaches to determine the presence of flooded areas, with a big effort toward the cloud and terrain shadow removal [11]. Since March 2018, the software has been delivered by CSPP in a version adapted for direct broadcast satellite receiving systems [44]. The software can process either full pass length SDRs by default or user defined latitude/longitude ROIs. The flood maps generated by VNG for the ROI shown in Figure 1 have been produced (Figure 5), considering the cloud-free VIIRS daytime imagery of the event. The output is a colour enhanced 8 bit GeoTIFF image with the main identified features differently depicted on the basis of the provided legend [44].

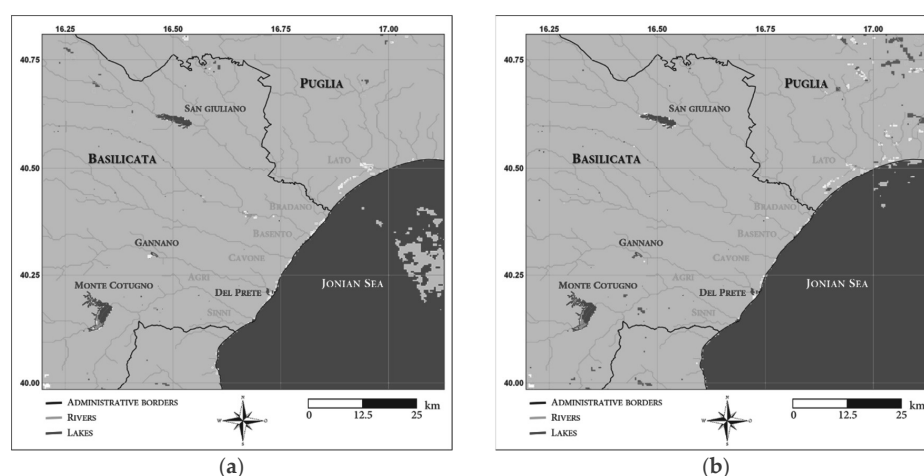


**Figure 5.** Cont.

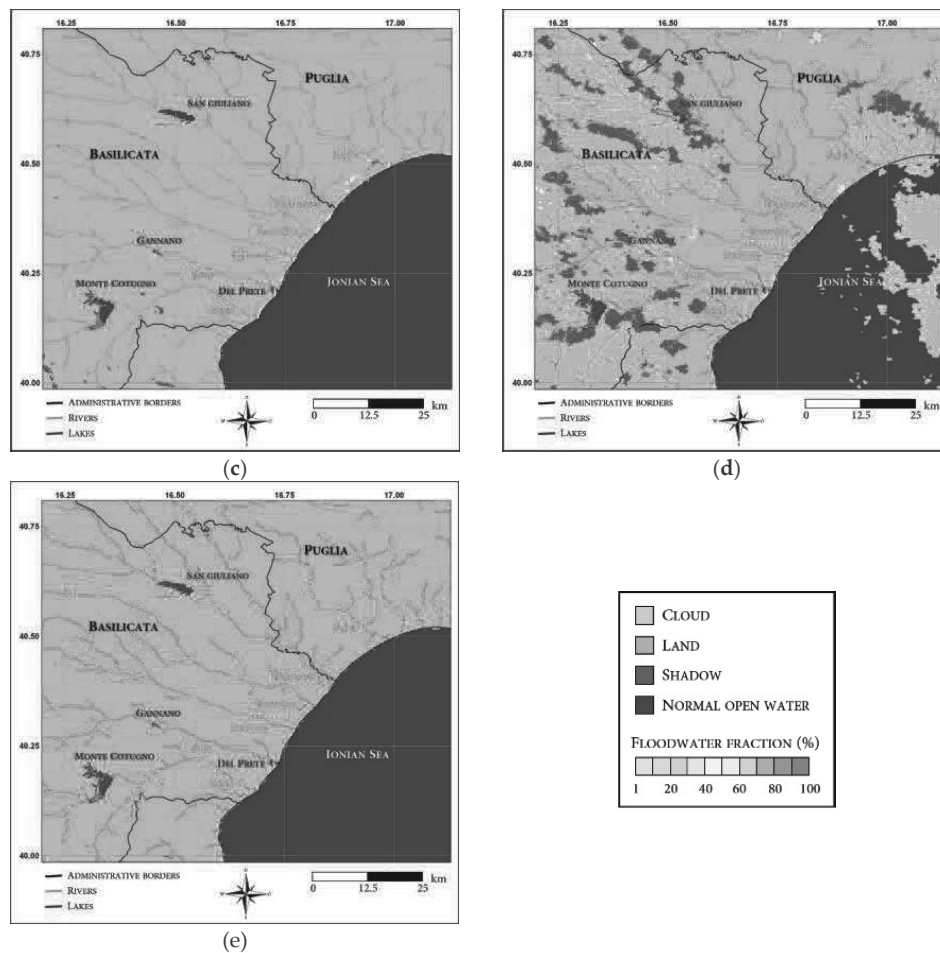


**Figure 5.** VNG products related to the ROI shown in Figure 1 for: (a) 04/12/2013 at 12:10 GMT; (b) 05/12/2013 at 11:52 GMT; (c) 06/12/2013 at 11:35 GMT; (d) 07/12/2013 at 11:12 GMT; (e) 08/12/2013 at 12:36 GMT.

### 3.3. The Robust Satellite Techniques (RST) Approach

RST is an automatic change-detection scheme, already applied with good accuracy in monitoring different natural and environmental hazards (see [21] and references herein). RST identifies statistically significant variations, at pixel level, for the signal under investigation by: (i) analysing multi-year time series of cloud-free homogeneous (same calendar month, same acquisition time, same spectral channel/s) satellite records; (ii) searching for anomalies by means of a specific change detection step. The latter exploits the “Absolute Variation of Local Change of Environment (ALICE) Index” defined as follows:

$$\otimes_V(x, y, t) = \frac{V(x, y, t) - \mu_V(x, y)}{\sigma_V(x, y)}, \quad (1)$$

where,  $V(x, y, t)$  is the signal measured at time  $t$  for each pixel  $(x, y)$  of the analysed satellite scene, while  $\mu_V(x, y)$  and  $\sigma_V(x, y)$  represent respectively the temporal mean and standard deviation (i.e., the reference fields), both computed by processing the above mentioned homogeneous multi-temporal dataset of satellite imagery” [22]. Such an index is, for its inherent design, a standardized variable that should show a Gaussian behaviour (i.e., mean  $\sim 0$  and standard deviation  $\sim 1$ ), therefore, the higher the absolute value measured, the lower the probability of occurrence [49]. Namely, the probability of occurrence of an anomalous signal decreases from about 4.5% for  $|\otimes_V| > 2$  (level of statistical significance) to 0.3% for  $|\otimes_V| > 3$  and even lower values for increased  $|\otimes_V|$  [30]. The analysis at pixel level of long-term signal series acquired under the same observation conditions (i.e., same sun height,